Journal of Building Engineering 112 (2025) 113786

Contents lists available at ScienceDirect

Journal of Building Engineering

journal homepage: www.elsevier.com/locate/jobe

Hemp-based systems as seismic strenghtening interventions of existing masonry buildings

Emilia Meglio, Antonio Formisano *

Department of Structures for Engineering and Architecture, University of Naples Federico II, Piazzale Tecchio 80, 80125, Naples, Italy

ARTICLE INFO

Keywords:
Natural fibres
Hemp
Masonry buildings
Seismic retrofit
FRP
FRCM

ABSTRACT

The work aims to illustrate three research issues dealing with the use of hemp for seismic strengthening of existing masonry buildings. Hemp fibres, thanks to their mechanical properties, represent a valid alternative to artificial ones in the context of environmental sustainability. Two types of reinforced plasters are herein investigated by means of laboratory tests: the first one is a plaster with hemp fibres randomly arranged in the matrix, while the second one is a plaster reinforced with a hemp mesh to obtain a Hemp Fibre-Reinforced Cementitious Matrix (H-FRCM). The last matter is a numerical study on the seismic behaviour of a masonry school building located in Southern Italy reinforced firstly with a Hemp Fibre Reinforced Polymer (H-FRP) and then with the experimented H-FRCM system. Both experimental campaigns display an increase of compressive and flexural strength of the used plasters due to the presence of hemp. Moreover, the hemp mesh allows to obtain a significant improvement of the collapse mode of the masonry. The increase in strength achieved from tests is also confirmed by the numerical analyses, even if with the H-FRCM reinforcement the seismic upgrading of the studied building is not achieved. As a conclusion, the gotten results show interesting perspective in the use of hemp fibres for reinforcement of masonry buildings under seismic viewpoint.

1. Introduction

In recent years, environmental sustainability has become a central concern, especially in the construction industry. The construction sector accounts for about 24 % of global raw material use and is responsible for approximately 35 % of primary energy consumptions and 38 % of CO_2 emissions, considering all phases from extraction to demolition [1]. To reduce the environmental footprint, research focused on developing sustainable building materials by modifying the production process or replacing traditional inputs with eco-friendly alternatives. Amont these, natural fibre composites (NFCs) have emerged as promising due to their minor environmental impact and low cost. Plant-based fibres are especially attractive for structural applications thanks to their high strength and stiffness [2]. Their use agrees with the development of agricultural activities and align with sustainable practice meeting the "Reuse-Reduce-Recycle" action [3]. Hemp shows substantial advantages compared to other natural fibres for its excellent thermal and acoustic insulation properties, low density, and mechanical resistance [4], since it is characterized by tensile strength of about 690 MPa, Young modulus of 30–60 GPa and failure strain of about 1.6 % [5]; [6]. From an environmental perspective, hemp cultivation has numerous advantages. As the plants are not damaged by insects and rodents, they do not require insecticides and pesticides. Furthermore, it has been shown that a hectare of hemp cultivation absorbs a quantity of CO_2 four times higher than a forest in the same

* Corresponding author.
E-mail address: antoform@unina.it (A. Formisano).

https://doi.org/10.1016/j.jobe.2025.113786
Received 8 August 2023; Received in revised form 10 July 2025; Accepted 15 August 2025
Available online 21 August 2025

area [7]. With a simple processing of its fibres, hemp can be employed in the production of bricks, blocks, panels, plasters, coats, and screeds used for a great variety of applications in new and old buildings [8].

Currently, the wide employment of natural fibres, including hemp, remains challenging. Many factors affect the mechanical performances of NFCs, including the selection of fibres and matrix, as well as their manufacturing process. The unsatisfactory reinforcement level reported by studies on natural fibres in comparison to artificial fibres, as glass, is often motivated by compatibility and adhesion issues between the fibres and the matrix. Investigations focused on improving the mechanical performance of hemp composites are still limited. Nevertheless, some studies on composite materials made of hemp fibres are reported with reference to mortars, concretes, and bricks. Comak et al. [9] studied cement mortars with 1–3 % hemp fibres (6–18 mm length), finding that 2–3 % fibre content with 12 mm length optimized compressive and flexural strength, without negatively affecting workability. Two studies examined pozzolanic-lime mortars reinforced with hemp fibre grids. Asprone et al. [10] showed that latex-coated fibres improved durability and fibre-matrix bond, with 4–6 grid layers enhancing flexural strength and ductility. Menna et al. [11] tested masonry panels with hemp-reinforced mortar on tuff and clay brick walls, reporting 2–5 times increases in shear strength and more uniform crack patterns under diagonal compression. Hemp concrete, made of hemp particles and binder, can significantly reduce environmental impact—storing about 35 kg CO_2/m^2 over 100 years [12]. Awwad et al. [3] replaced 10–30 % of aggregates with hemp fibres (0.5–1 %), finding reduced workability and compressive strength, but improved ductility. Merta & Tschegg [13] tested concrete with 0.19 % natural fibres (hemp, elephant grass, wheat straw) and found hemp improved fracture energy by 70 %, due to good fibre-matrix bonding. Other studies investigated hemp-based composite blocks. Dubois et al. [14] developed non-load-bearing hemp concrete blocks using quarry fines and hemp straw, achieving strength comparable to gypsum or cellular blocks, with improved acoustic absorption. Zak et al. [15] studied earth bricks reinforced with hemp and combined with gypsum/cement. While hemp reduced compressive strength slightly, it significantly enhanced ductility, demonstrating its potential to improve material behavior despite reduced density.

In the present research, two experimental campaigns on possible use of hemp as structural reinforcement of masonry structures are conducted. The first research is about laboratory tests performed on a plaster reinforced with hemp fibres under forms of braids randomly added in the mixture, whereas the second activity is still a laboratory test on a plaster reinforced with a hemp mesh. In conclusion, it is presented a numerical application of two hemp-based systems, namely a Hemp Fibre-Reinforced Polymer (H-FRP), made of hemp fibres and resins, and a Hemp Fibre-Reinforced Cementitious Matrix (H-FRCM), made of hemp fibres and a lime matrix, for seismic strengthening of an existing masonry building.

2. Lime-based plaster reinforced with random hemp fibres

After the above literature review, some experimental tests were performed to investigate other hemp sub-products to be used for reinforced sustainable plasters. In particular, an experimental campaign was carried out on a lime-based plaster reinforced with hemp fibres randomly arranged in the mixture. The plaster was investigated by means of physical and mechanical tests to assess the influence of the hemp fibres on the behaviour of the studied anti-seismic mortar. In fact, the results were compared to the ones obtained for the unreinforced sample called “Control”. The capacity of water absorption of the hemp braids was assessed to determine the water/lime ratio of the compound. Then, three reinforced mixtures were prepared and subjected to workability tests. The last phase regarded the determination of the mechanical performances by means of bending and compressive tests.

2.1. Materials properties

The control specimen is manufactured with a fine-grain structural geo-mortar made from pure natural NHL range and geo-binder. The mortar falls into the resistance class M15 according to the EN 988-2 standard, and R1, according to the EN 1504-3 standard. Additional information on the pre-mixed mortar, contained in technical data sheet provided by the producer, are summarized in Table 1.

Hemp fibres were included in the matrix under form of braids deriving from a hemp fabric produced in Italy from a local cultivation (Fig. 1). The diameter of the braids was equal to 0.4 mm. These hemp fibres were cut in two different lengths of 2 and 3 cm and added in the blend in five percentages in weight of pre-mixed from 0.25 % to 1.5 %.

2.2. Absorption capacity tests

The preliminary phase of the experimental campaign saw the absorption capacity test to assess the water absorption capacity of the hemp braids. The test was carried out by soaking a defined quantity of fibres (10 g) in a glass of water and, subsequently, by weighting the fibres every 15 min for the first 2 h, then after 12 h, 24 h and every day for the next 6 days. Before weighing, wet fibres were drained

Table 1
Technical data of the premixed geo-mortar.

Mixing water	5.3 L/bag (1 bag = 25 kg)
Compressive strength (after 28 days)	>15 MPa (EN 998-2)
Flexural tensile strength (after 28 days)	>5 MPa (EN 196/1)
Modulus of elasticity under compression (after 28 days)	9 GPa (EN 13412)

Fig. 1. Hemp fabric (a) and cut hemp fibres (b).

and laid on a paper towel to remove excessive and superficial water. The difference between the soaked weight and the initial weight returned the variation of weight of the fibres due to the absorption of water. The test was necessary to assess the amount of water to be added in the blend to maintain the optimal water/lime ratio suggested from the producer to guarantee an adequate workability and resistance of the pre-mixed product. The results of the tests are graphically depicted in Fig. 2.

The most relevant result of the test was that, even if the curve became almost stable at a value of 440 % of the initial weight after the first day, the larger quantity of water (43 g of water compared to the 44.6 g at the end of the test) was absorbed by the fibres in the first 2 h of immersion. Therefore, it was decided to add the fibres in the blend already saturated after 2 h of immersion in water.

2.3. Workability tests

The reinforced plaster was investigated with different combinations of mortar and hemp fibres to be always compared to an un-reinforced mortar without fibres. The original plan for the mix designs was to add fibres in the blend with two different length (2 and 3 cm) and with eight percentages in weight of pre-mixed material (0.25 %, 0.50 %, 0.75 %, 1.00 %, 1.50 %, 2.00 %, 2.50 % and 3.00 %). Nevertheless, after these tests, specimens with some percentages of fibres were discarded due to absence of workability. Each mixture was labelled with an identification code that summarises the main characteristics: resistance class of the mortar, length of the hemp fibre, percentage of hemp fibres. For example, the mixtures made of M15 mortar with 0.50 % of hemp fibres having length of 2 cm are labelled as M15_2_0.50 %. The control specimen (without fibres) was identified as M15_CNTL.

The workability test of the mixture was performed with the shaking table according to UNI EN 1015-3 standard. It allowed to measure the spread of the mortar after the flow provoked by 15 shakes in 15 s and directly relate the so-called spreading diameter to the mortar consistency (Fig. 3). The spreading diameter of the mortar was obtained as average value of two orthogonal diameters measured from the tests.

Fig. 4 illustrates the test results in terms of spreading diameter measured for the specimens manufactured with the two investigated lengths and variable percentages of hemp. The results were compared to the workability of the control specimen and to the following reference range of the spreading diameter (Sp) suggested by the UNI 998-1/2:2016 standard:

$$140\ mm < Sp < 180\ mm\ (\pm\ 10\ mm\ of\ tollerance)$$

which allows to have a good workability of tested plasters.

The spreading diameter of the control specimen was found to be equal to 140 mm, which is the lowest admissible value allowed for plasters. The workability of both mixtures with percentages of hemp addition lower than 0.5 % was higher than the control sample, but when increasing the percentages of hemp, the workability decreased. For percentages of hemp higher than 1 % the mortar did not fall within the limits of the suggested range. Therefore, it was chosen to disregard specimens with hemp having percentages greater than 1.5 % in the absorption capacity test.

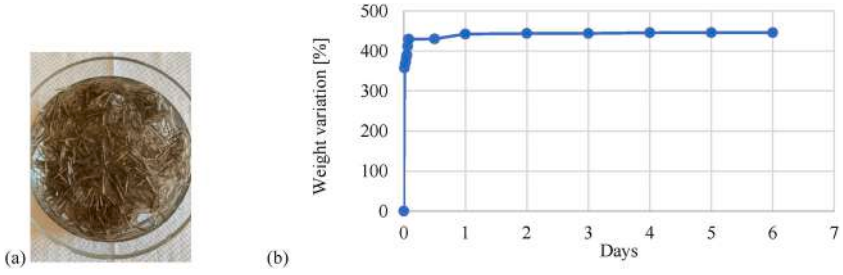

Fig. 2. Absorption capacity test on 0.4 mm hemp fibres (a) and results (b).

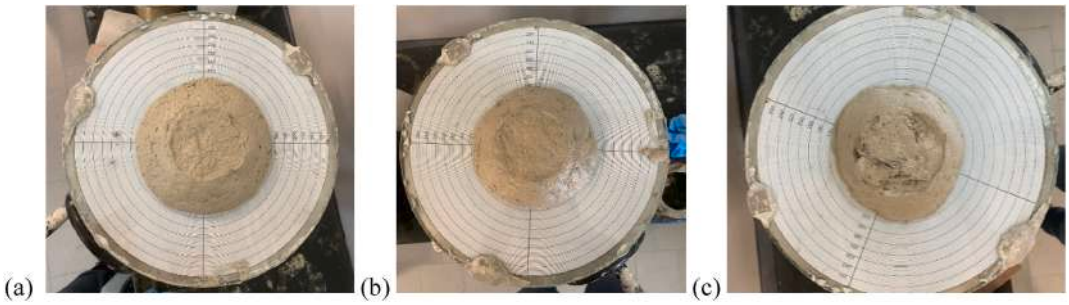

Fig. 3. Workability tests on reinforced plasters made of 0.75 % (a) 1 % (b) and 1.5 % (c) of hemp fibres.

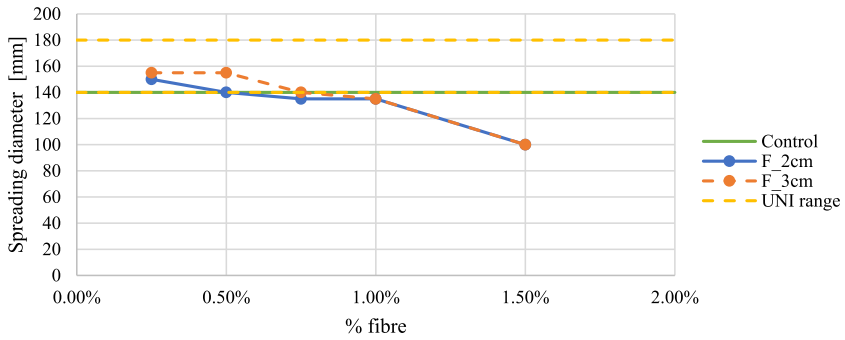

Fig. 4. Workability test: spreading diameters of hemp reinforced plaster.

2.4. Mechanical tests

The mechanical properties were investigated only for the mixtures exhibiting the best behaviour during the workability. Therefore, only the samples with 0.25 % and 0.50 % of hemp fibres having both the two examined lengths (2 and 3 cm) were inspected. Three prismatic (40 × 40 × 160 mm) and three cubic (40 × 40 × 40 mm) specimens were manufactured for each mixture according to the procedures described in the UNI EN 196-1 standard.

2.4.1. Bending test

The tensile strength of the mortar was assessed by means of three-point bending tests according to the UNI EN 772-1 and UNI EN 772-2 standards on the 40 × 40 × 160 mm specimens (Fig. 5).

The output of the test is a force-time curve, where the tensile failure strength due to bending (f_{cf}) of the mortar was calculated. The results in terms of tensile strength are depicted in Fig. 6 for each specimen, where it is also highlighted the average value of the three specimens for each mixture ($f_{cf,\ av}$) and the coefficient of variation (CV).

From tests it was apparent that the average value of the tensile strength is always higher for the reinforced mixtures compared to the control one (without fibres), which is highlighted in the previous histogram with a dashed red line. The most relevant increase was obtained for the plaster with 0.5 % of hemp fibres with a length of 2 cm, for which the tensile strength was found to be around 81 % higher than the tensile strength of the traditional geo-mortar. In the other mixtures, the increase in tensile strength due to bending is

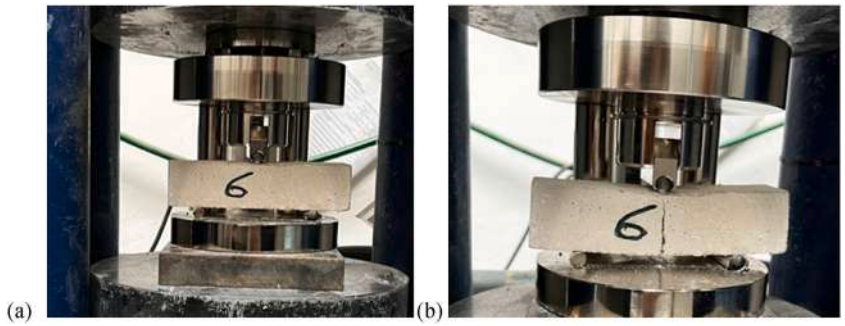

Fig. 5. Three-point bending test: initial phase (a) and collapse (b).

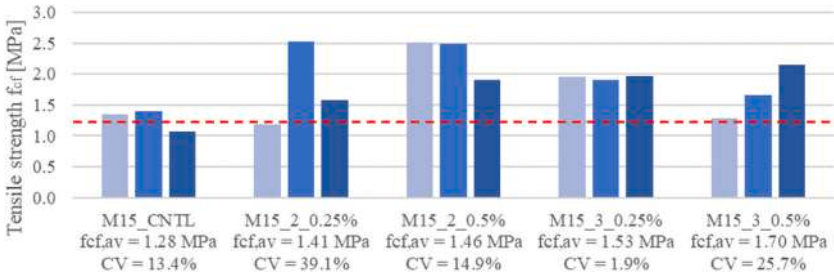

Fig. 6. Results of three-point bending tests in terms of tensile strength due to bending f_{cf}. (red dashed line: average strength of the control specimen).

equal to 38 % (M15_2_0.25 %), 52.3 % (M15_3_0.25 %) and 33 % (M15_3_0.50 %).

The influence of hemp fibres on the elastic modulus of the mortar is depicted in Fig. 7 for each specimen, where it is also highlighted the average value of the three specimens for each mixture ($E_{,av}$) and the coefficient of variation (CV).

2.4.2. Compressive test

The compressive strength of the mortar was assessed by means of compressive tests according to the UNI EN 772-1 and UNI EN 772-2 standards. The test was performed after 28 days of curing on 40 × 40 × 40 mm specimens using the same machine used for bending tests. The output of the test is a force-displacement curve, from which it was computed the compressive failure strength (σ_c) and the strain (ε) of the mortar. The results in terms of tensile compressive strength are depicted in Fig. 8 for each specimen, where it is also highlighted the average value of the three specimens for each mixture ($\sigma_{c,av}$) and the coefficient of variation (CV).

From the performed tests, it was noticed that average value of the compressive strength is always higher in the reinforced mixtures compared to the control one (without fibres). The percentage increase is around 11–23 % for the reinforced mortar, and the best behaviour was found for the specimens with 2 cm long fibres. Furthermore, the fibres provide a confinement effect to the mortar (Fig. 9) that also allows to reach higher values of strain.

The influence of hemp fibres on the elastic modulus of the mortar is depicted in Fig. 10 for each specimen, where it is also highlighted the average value of the three specimens for each mixture ($E_{,av}$) and the coefficient of variation (CV).

3. Lime-based plaster reinforced with hemp mesh

Hemp fibres can also be arranged in form of a mesh to obtain a seismic strengthening system similar to the classical Fibre Reinforced Cementitious Matrix (FRCM) one. This system is characterized by an inorganic matrix where one or more layers of hemp meshes are drowned to obtain a strengthening technique for masonry or reinforced concrete structures.

The second experimental campaign was carried out on a lime-based plaster reinforced with a hemp mesh. Two preliminary tests were carried out on the hemp fibres to evaluate both the capacity of water absorption and the tensile strength of the fibres, conformed under form of braids. In the preliminary phase different diameters of hemp braids were assessed to identify the optimal diameter to be used for the mesh. Afterwards, two specimens were manufactured to be subjected to compressive tests. The specimens were represented by two masonry walls, the first simply plastered on both sides and the second reinforced with the hemp mesh drowned between the two layers of plaster.

3.1. Properties of materials

The support wall manufactured with solid bricks having dimensions of 12 × 25 × 5.5 cm, compressive strength of 38.15 N/mm^2 and density of 1681 kg/m^3. Bricks were joined by a shrinkage-compensated hydraulic cementitious mortar with finely graded selection of aggregates and a binder typical of hydraulic cements (e.g., calcium silicates and aluminates). According to the technical data, the

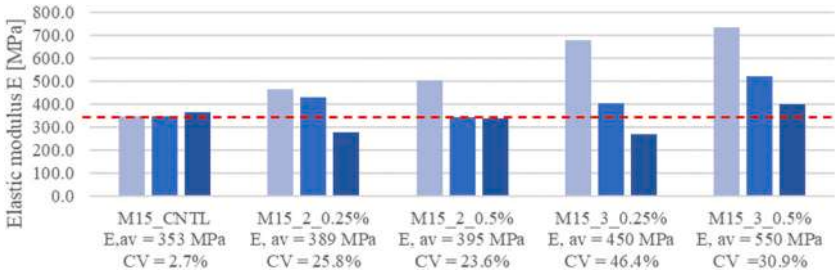

Fig. 7. Results of bending tests in terms of elastic modulus.

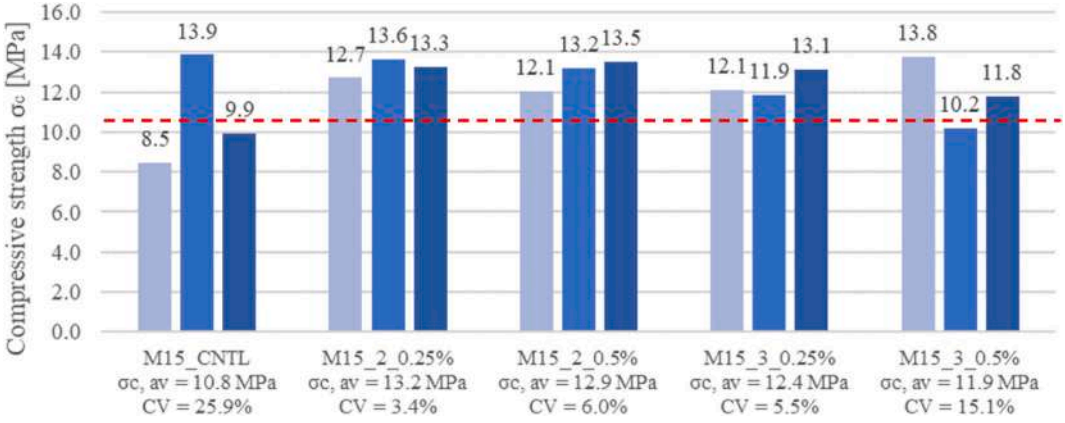

Fig. 8. Results of compressive tests in terms of ultimate strength (red dashed line: average strength of the control specimen).

Fig. 9. Specimens after compressive strength.

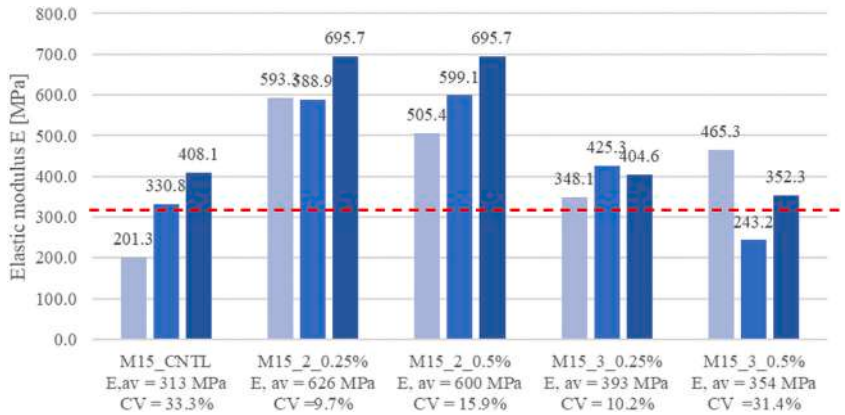

Fig. 10. Results of compressive tests in terms of elastic modulus.

mortar has a compressive strength of 18.17 N/mm^2 and a tensile strength of 1.44 N/mm^2, confirming its suitability for masonry applications.

The plaster was realized by using the same pre-mixed mortar used in the previous experimental campaign and it was placed on both sides of the specimens. Finally, the reinforcement was constituted by hemp fibres under form of braids with diameter of 2 mm which were derived from local cultivations.

3.2. Tensile test on hemp braids

Four diameters of hemp braids (1 mm, 2 mm, 3 mm and 4 mm) were tested to determine their tensile strength and to select the braid to form the mesh of the FRCM system. For each diameter, six samples were examined using a universal displacement control machine

according to the ASTM C1557 standard [16]. The load application rate was set at 2 mm/min and the data acquisition rate was 10 Hz. The length of samples was 700 mm to allow an anchorage length to the machine of 100 mm to assess the elongation over a reference length of 500 mm (Fig. 11).

The output of the uniaxial tensile test is a force-displacement curve, which allowed to obtain a stress-strain diagram where the strains were monitored using digital video extensometer based on optical tracking of markers applied directly to the specimen. The results for all the investigated diameters are depicted in Fig. 12, where the samples are identified as D1, D2, D3 and D4 respectively for the diameters of 1, 2, 3 and 4 mm. In the histogram, the values of stress represent the average values among those of the three samples tested for each diameter.

From the test it was observed that the tensile strength reached the maximum value of 155.3 MPa (D1) and a minimum value of 27.3 MPa (D3). The variation in tensile test results among the four braid diameters can be attributed to differences in the manufacturing process. Specifically, in the first case (D1 and D3), the braids are composed of a single strand, whereas in the second case (D2 and D4), they are constructed from multiple strands. The hemp mesh was fabricated using a multi-strand braid with intermediate mechanical properties. Specifically, the 2 mm diameter braid (D2) was selected, which exhibited an average tensile strength of 68.2 MPa.

3.3. Absorption capacity tests

The preliminary phase of the experimental campaign also saw the execution of tests to assess the water absorption capacity of the selected hemp braid. The test was performed following the same procedure adopted in the previous experimental campaign on three samples of 2 mm hemp braids (D2). The results of the absorption capacity tests are graphically depicted in Fig. 13.

Also in this case, the larger quantity of water was absorbed by the fibres in the first 2 h of immersion, so that it was decided to add the mesh already saturated of water in the plaster. The total amount of water absorbed by the fibres was around 1.27 times their weight at the end of the saturation process with a coefficient of variation (CV) of 3.04 %.

3.4. Compressive test

After the preliminary test, the unreinforced and reinforced specimens for the compressive test were manufactured. The support wall, having dimensions of 50 × 50 cm with a thickness of 12 cm, is the same for both samples. It was built with solid bricks placed with staggered joints having a thickness of 1 cm. The specimen construction was facilitated by using a wooden formwork in which the preliminary wetted bricks were inserted and connected to each other by means of a controlled-shrinkage mortar. After the curing process of the mortar joints, the unreinforced specimen (Control_01) was simply plastered on both sides with two layers of pre-mixed mortar, each of them having thickness of 1.5 cm. The reinforced specimen (Reinf_01) was also made of two layers of plaster, of 1.5 cm each, in which the hemp mesh was drowned. The mesh was realized with hemp braids having a diameter of 2 mm and arranged to have a spacing of 20 × 20 mm. The joints between horizontal and vertical braids were fixed with a polyvinyl acetate adhesive to provide an acceptable stiffness to the mesh to be lifted and placed on the wall after 2 h of immersion in water, as suggested by the absorption capacity test. The mesh was furtherly fixed to the wall with four mechanical anchors inserted in preset holes executed on the wall at 8 cm from the edges to avoid any damage of the bricks. The last phase of the sample preparation was the regularization of the end cross-section of the walls in contact to the machine with a hi-flow mortar to obtain a perfectly smooth surface. The phases of specimens manufacturing are graphically illustrated in Fig. 14.

Each specimen was equipped with four vertical transducers (two for each face) to monitor the displacements in the loading direction and two horizontal transducers (one for each face) to check the horizontal movements. The instruments were positioned to create a 20 × 20 cm square centered in the centre of the wall (Fig. 15).

Once the preparation of the samples was completed, the specimens were tested under compression with a universal displacement-controlled machine having a load capacity of 1000 kN according to the UNI EN 12390-3 standard. The machine output is a force-displacement curve, in which the displacement is registered as average value between the ones recorded from the vertical transducers. Fig. 16 illustrates the force-displacement diagram of the unreinforced (Control_01) and reinforced (Reinf_01) specimens and

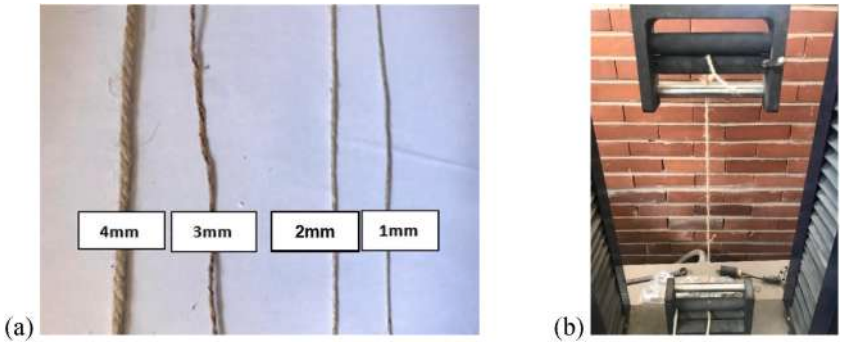

Fig. 11. Samples of hemp braids for the tensile test (a) and 4 mm braid during testing phase (b).

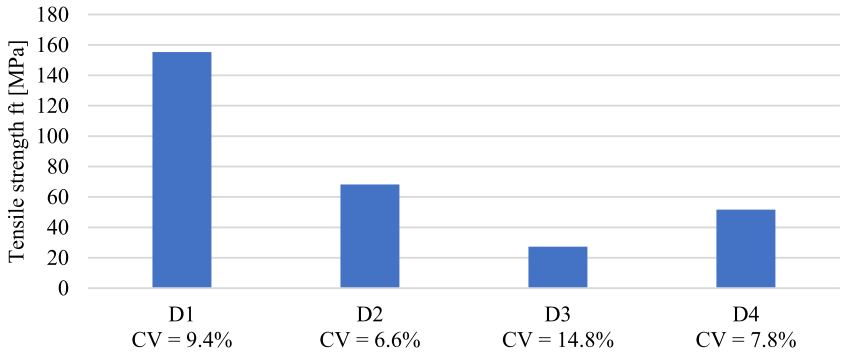

Fig. 12. Average tensile strength of hemp braids (CV = Coefficient of Variation).

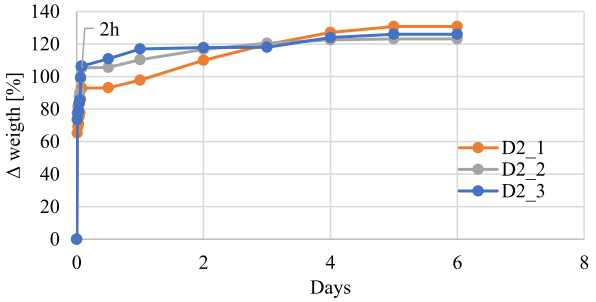

Fig. 13. Results in terms of variation of weight of the absorption capacity test on 2 mm hemp fibres.

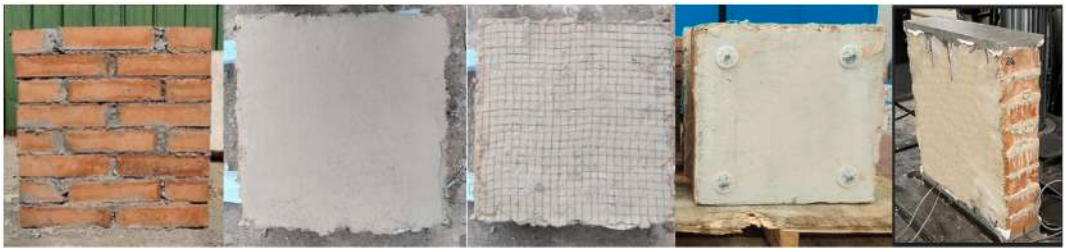

Fig. 14. Manufacturing phases of the reinforced wall (Reinf_01) and regularization of the end cross-sections.

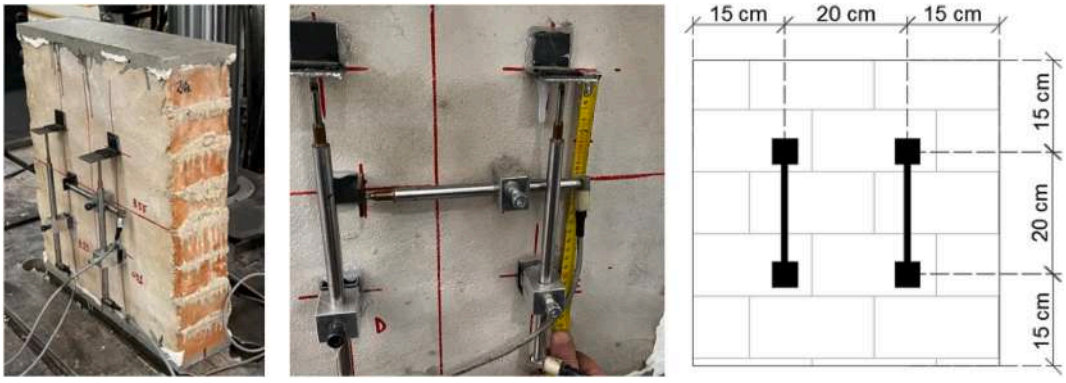

Fig. 15. Application of the transducers for the compressive test.

the values of the maximum force attained and the related displacements measured by the vertical transducers.

From the performed tests, it was perceived that the hemp mesh allowed to reach an increase of maximum force of around 13.6 % and an increase of 4.5 % of the related displacement compared to the corresponding properties of the unreinforced specimen. The most relevant result obtained from the experimental campaign was the difference between the collapse modes of the two investigated specimens. In fact, the unreinforced wall showed both several vertical cracks in the bricks and the plaster layers totally detached from both masonry sides. On the other side, the reinforced wall only exhibited a capillary crack pattern, without suffering large lesions in the bricks as in the previous case. Moreover, the hemp mesh and the mechanical anchors also prevented the out-of-plane failure of the plaster (Fig. 17).

Although the present experimental campaign focused on the global compressive response of masonry panels, the observed increase in maximum load and the improved crack pattern also suggested an enhanced shear behavior due to the presence of the hemp mesh. In this regard, several analytical models are available in the literature for predicting the shear strength of masonry walls retrofitted with FRCM systems [17]; [18,19], which could serve as a reference for interpreting and validating the achieved experimental results.

4. Seismic strengthening of an existing building with hemp fibres

In the last section of the research, two applications of seismic strengthening by hemp fibres of an existing masonry building are presented. The reference building is the Massaia Institute in San Giorgio a Cremano (Naples) in the Campania region of Italy. It is a secondary school building articulated in two separate blocks: the first (Body A) has a load bearing masonry structure developed on two levels, which is the actual school, while the second (Body B) has a reinforced concrete structure used to host the school gym (Fig. 18). The reinforcement with hemp systems will be applied to the masonry structure (Fig. 19), that will be the only structure considered in the following paragraphs.

This structure was globally analysed with the TreMuri structural software before and after the application of two types of hemp reinforcements based on FRP and FRCM systems. To create a representative model of the existing structure, it was necessary to collect all the available information about the material properties, the geometries and the loading conditions of the structure that will be described in the following sections along with the results of the seismic analyses before and after the interventions. All these data were acquired by in-situ surveys to confirm the available documentations of the original project.

4.1. Materials and geometries

The geometrical and structural configuration of the masonry structure, together with the mechanical properties of structural materials, were collected through on-situ surveys. In particular, non-destructive and partially destructive investigations, such as thermographic tests and double flat jacks, were performed on masonry walls to attain an extensive knowledge level of the building. From the survey it was noted that the in-elevation masonry structure is made of Neapolitan yellow tuff walls with variable thickness from 55 mm to 65 cm and with a good level of clamping among orthogonal walls. The floors of both levels are made of on-site casted RC joists, which are connected to the walls via RC ring beams having the same thickness of perimetral walls. The foundations, made of volcanic stones, are obtained from an enlargement of the in-elevation masonry walls and presented a height of around 2.20 m. According to the Italian regulations, the masonry structure falls into two categories: soft stone masonry made of tuff bricks for the in-elevation structure, whose properties were deducted from on-situ inspections, and split masonry with stones assembles with good texture for the foundations, whose mechanical properties were taken as medium values of the range provided by the Table C8.5. I of the Italian Circular No. July 2019 [20]. For the tuff masonry walls, an extensive Level of Knowledge (LC2), which correspond a confident factor of 1.20 to, was achieved; contrary, for the volcanic stone masonry, a limited Level of Knowledge (LC1), which correspond a confident factor of 1.35 to, was attained. Tables 2 and 3 show the mechanical parameters used in the calculation software according to the knowledge level attained for each structural material.

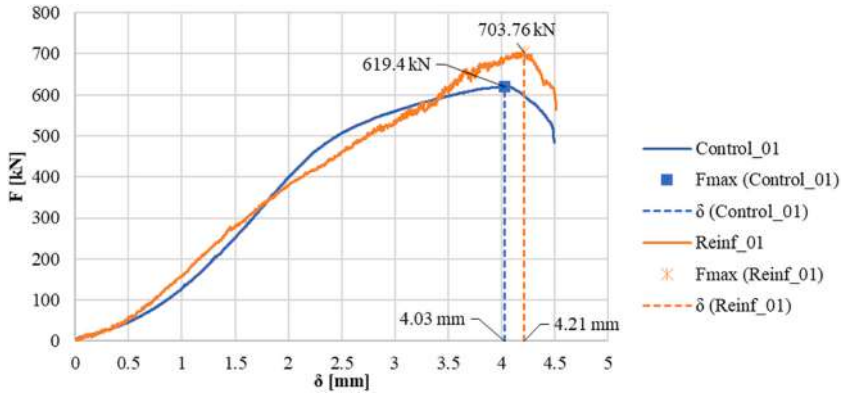

Fig. 16. Force-displacement compressive curves on the unreinforced and reinforced walls.

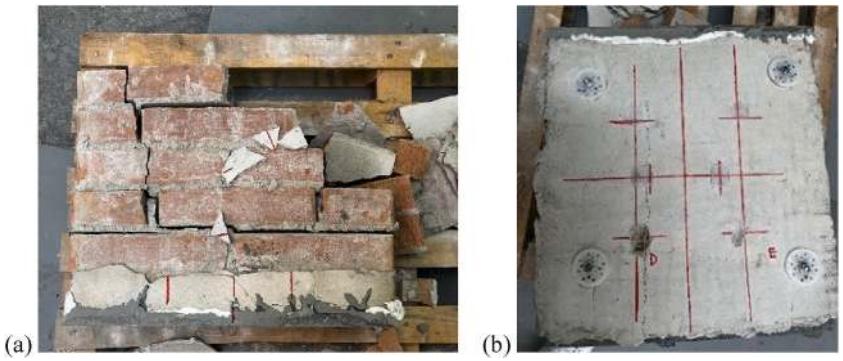

Fig. 17. Crack patterns of the unreinforced (a) and reinforced (b) walls after compressive test.

Fig. 18. Localization of the case study: the Massaia Institute of San Giorgio a Cremano (district of Naples).

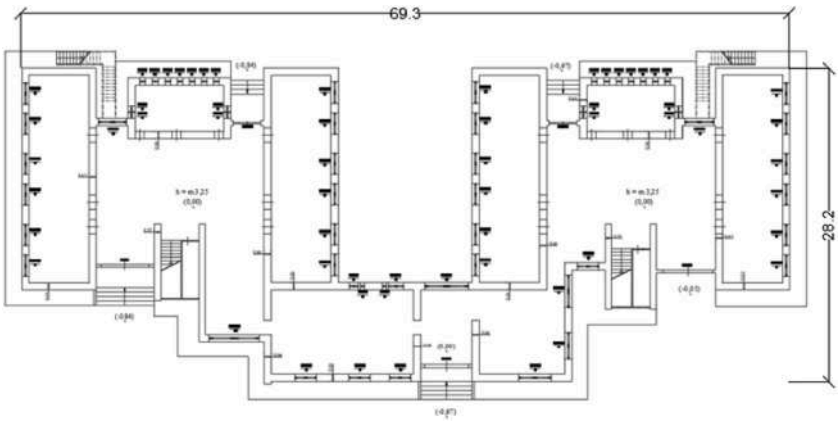

Fig. 19. Body A: plan layout of the first level (measurement unit: m).

4.2. Structural model and seismic analysis

The structural model of the existing masonry building was implemented in the software TreMuri, which is calculation software specific for masonry structures. developed by the S.T.A. data company. The software is based on the Frame by Macro Element method

Table 2
Mechanical properties of soft stone masonry made of tuff bricks (FC = 1.20).

Characteristics	Value
Medium compressive strength (f_m)	2.24 MPa
Medium shear strength (τ_0)	0.06 N/cm^2
Normal modulus of elasticity (E)	2090 MPa
Tangential modulus of elasticity (G)	667 MPa
Partial safety coefficient for compressive strength (Υ_M)	3

Table 3
Mechanical properties of split masonry with assemblage of stones having good texture (FC = 1.35).

Characteristics	Value
Medium compressive strength (f_m)	2.60 MPa
Medium shear strength (τ_0)	0.056 MPa
Normal modulus of elasticity (E)	1740 MPa
Tangential modulus of elasticity (G)	580 MPa
Partial safety coefficient for compressive strength (Υ_M)	3

[21]; [22]), which involves discretising the walls into two macro-elements (piers and spandrels) connected to each other by rigid nodes, that represents the portion of the structure less prone to seismic damages.

In the modelling phase of the school building, it was used the Turnšek– Cacovic model for the masonry walls. All the structural elements considered capable of resisting to vertical and horizontal actions were implemented in the calculation software taking into account the dimensions and location of openings. Fig. 20 illustrates the three-dimensional view of the structure implemented in the TreMuri software and a view of the macro-element model.

Before and after the interventions with hemp fibres, the following types of analysis were performed on the structure.

- Linear static analysis for checks under gravity loads;
- Linear kinematic analysis for checks related to local failure mechanisms;
- Non-linear static analysis to assess the global seismic behaviour of the school building.

It was also performed a preliminary investigation based on modal analysis to assess the vibration modes of the structure. To focus on the influence of the two types of hemp reinforcement, in the following the analysis results before and after the intervention in terms of modal shapes and global seismic behaviour will be reported. In addition, the effectiveness of the reinforcement types will be assessed in terms of seismic risk classification.

4.3. Results of seismic analysis on the unreinforced structure

The modal investigation allowed to identify the modal shapes and the participating mass of each vibration mode of the existing structure. The first vibration mode was in the longitudinal direction (X) with a participating mass of around 86 %, while in the transverse direction (Y) the first significant mode is the fourth with a participating mass of around 79 %. This data allowed to perform a pushover analysis on the structure according to the Italian regulations, that sets a minimum participating mass in the main direction of 60 % for masonry buildings to perform non-linear static analyses. The results of the modal investigation on the unreinforced structure are summarized in Table 4 for the first 9 vibration modes.

The global seismic behaviour was assessed by means of a pushover analysis according to two distribution of inertia forces: proportional to static forces and as uniform distribution of accelerations over the structure height. For each distribution, load cases were defined for two directions of earthquake (X and Y) and different accidental eccentricities, reaching a total number of 24 pushover analysis. The pushover curve plots the seismic base shear versus the displacement of a control node that was chosen, according to the Italian code [23], in a barycentric position at the top level (node 130 in Fig. 21). Furthermore, due to the irregular configuration of the structure, nodes 142 and 127 were also monitored to evaluate the variation of the analysis results and select the most reliable node for subsequent evaluations.

The analysis was stopped when the 80 % decay of the base shear was attained. The results of the seismic analysis in terms of pushover curves are illustrated in Fig. 22.

The global seismic analysis allowed to compute the seismic risk safety index, that represents the ratio between the capacity seismic action that the structure is able to withstand and the one required for a new building according to the Italian regulations (NTC, 2018). The school building showed the worst behaviour in the longitudinal direction (X), attaining the lowest value of the seismic risk safety index of 0.59. It means that the building is able to withstand only 59 % of the seismic actions required to new buildings at the Life Safety Limit State. The damages occurred in the masonry walls in the most severe load combination are shown in Fig. 23 with an appropriate scale of colours (dark green = incipient plasticity; pink = compressive-bending plastic; magenta = serious crisis; yellow = shear plastic; orange = incipient shear failure; dark orange = shear failure), where green and grey represent the absence of any damage. The results showed the most relevant collapses of the masonry panels at the top storey due to compression-bending and shear mechanisms.

4.3.1. Seismic risk classification according to Italian Guidelines 2017

To conclude the seismic assessment of the unreinforced building it was computed the seismic risk class according to the Italian Guidelines [24]. The guidelines provide operational tools for the classification of the seismic risk of construction which is divided into 8 classes from the lowest risk class (class A+) to the highest one (class G). The final seismic risk class is derived from the worst condition between an economic parameter (PAM Class) and a safety parameter (IS-V Class). PAM represents the Expected Average Annual Loss including the economic losses related to damages that can occur to structural and non-structural elements and the repairing cost of the

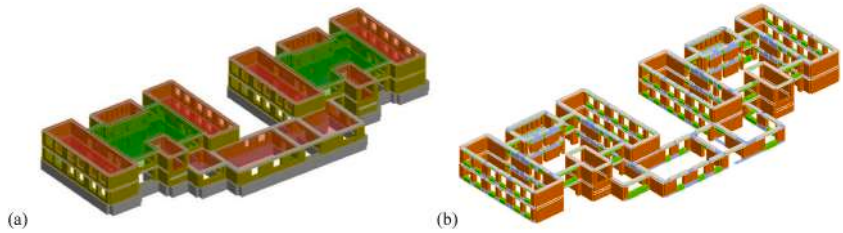

Fig. 20. Structural model (a) and macro-element model (b) of the school building (Body A) implemented in the TreMuri software.

Table 4
Modal analysis on the unreinforced structure.

Mode	T [s]	mx [kg]	Mx [%]	my [kg]	My [%]	mz [kg]	Mz [%]
1	0.23777	2.583.456	**86.02**	35	0.00	0	0.00
2	0.21297	11	0.00	48.636	1.62	0	0.00
3	0.19674	13.682	0.46	10.722	0.36	1	0.00
4	0.18234	26	0.00	2.368.538	**78.86**	30	0.00
5	0.17285	4.341	0.14	160.090	5.33	21	0.00
6	0.16274	3.423	0.11	54.892	1.83	65	0.00
7	0.11515	385.897	12.85	176	0.01	20	0.00
8	0.09681	199	0.01	3.727	0.12	1	0.00
9	0.08988	4.139	0.14	311	0.01	7	0.00

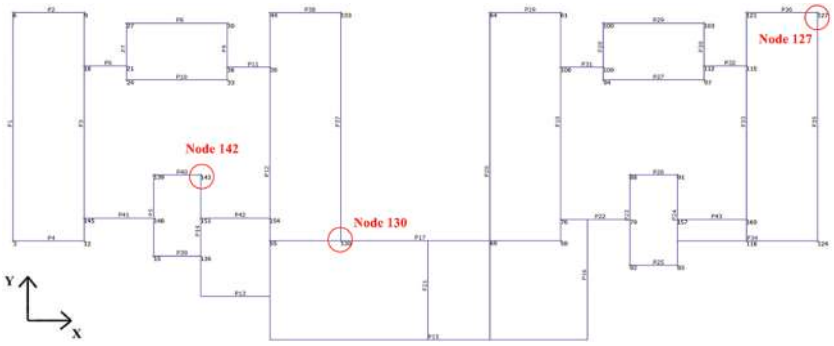

Fig. 21. Selected control nodes for the pushover analysis.

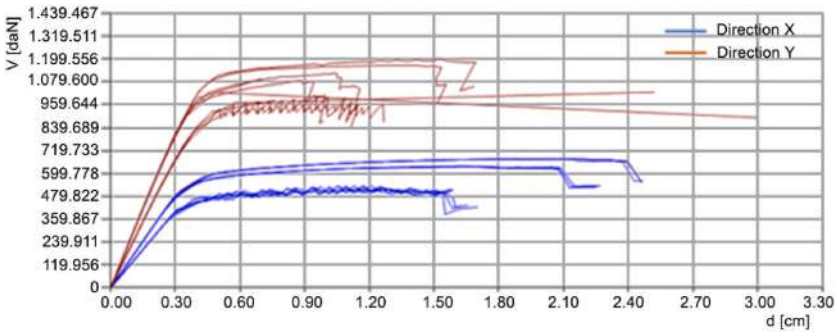

Fig. 22. Pushover curves of the unreinforced school building (Body A).

building after an earthquake as a percentage of the reconstruction cost. IS-V is the safety index of the structure which is defined as ratio between the capacity and the demand in terms of peak ground acceleration which was already assessed in the pushover analysis. For each parameter the seismic class is computed according to the values of Table 5 and the lowest class represent the seismic risk class of the building.

From the analysis it was saw that the unreinforced building has a seismic risk class C according to both parameters, which means

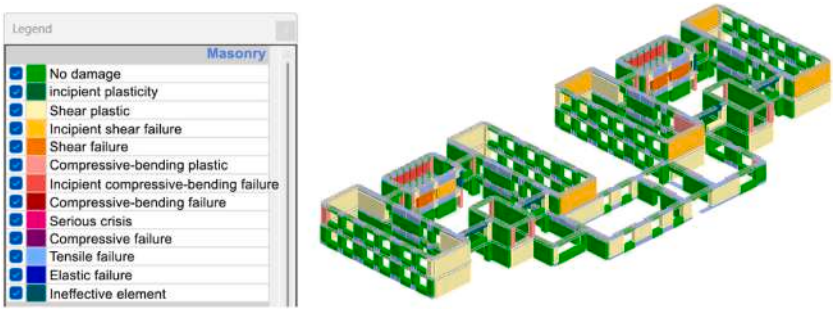

Fig. 23. Damages of the unreinforced school building (Body A) in the most severe load combination (Dir. X).

that the safety index is included between 45 % and 60 % of the seismic action and the PAM is in the range between 1.5 % and 2.5 % as shown in Table 6.

4.4. Seismic strengthening of the existing building

Two types of seismic strengthening interventions were applied to the masonry walls to assess the capacity of hemp fibres to seismically upgrade the performances of the studied school building. The seismic analyses on the building were repeated once reinforcement with either H-FRP or H-FRCM was made. In both cases the reinforcement was applied in an extensive way on the unreinforced buildings based on previous results of the same intervention but with artificial fibres that allowed to reach the minimum seismic risk class [25]. The walls interested by the reinforcement are reported in red in Fig. 24.

4.4.1. Hemp-based FRP retrofit system

Fibre-Reinforced Polymers (FRP) represent a reinforcement material made of fibres impregnated in a polymer matrix, that guarantees both the distribution of the loads between the fibres and the adhesion to the support [26]. The FRP retrofit system under consideration is made of hemp fibres and it is based on a product manufactured by an Italian company. It is a pre-impregnated fabric, having a weight-to-surface ratio of 380 g/m^2, balanced 50/50 % by weight of yarn. Its mechanical parameters are reported in Table 7.

The system was applied on the masonry walls with horizontal and vertical bands arranged in three layers, each having a thickness of 0.3 mm. The bands have a width of 30 cm and pitch of 50 cm in both directions, as depicted in Fig. 25.

The modal investigation was carried out and showed a similar behaviour to that of the unreinforced building. The global seismic behaviour was assessed by means of pushover analyses using the same 24 load combinations described for the unreinforced building. The results of the seismic analysis in terms of pushover curves are illustrated in Figs. 26 and 27, respectively, for direction X and Y in the most severe conditions.

The lowest value of seismic risk safety index after the retrofit with the H-FRP system was attained in the X direction with a value of 0.72, so providing a safety increase of 0.13 compared to that of the unreinforced building (seismic risk safety index = 0.59). The damages occurred in the masonry walls in the most severe load combination are shown in Fig. 28.

Table 5
Seismic risk classification according to the 2017 Italian Guidelines.

Safety Index	IS-V Class
100 % < IS-V	A^{+}_{IS-V}
80 % ≤ IS-V < 100 %	A_{IS-V}
60 % ≤ IS-V < 80 %	B_{IS-V}
45 % ≤ IS-V < 60 %	C_{IS-V}
30 % ≤ IS-V < 45 %	D_{IS-V}
15 % ≤ IS-V < 30 %	E_{IS-V}
IS-V ≤ 15 %	F_{IS-V}
100 % < IS-V	A^{+}_{IS-V}
80 % ≤ IS-V < 100 %	A_{IS-V}
Expected Average Annual Loss	**PAM Class**
PAM ≤0.50 %	A^{+}_{PAM}
0.50 % < PAM ≤1.0 %	A_{PAM}
1.0 % < PAM ≤1.5 %	B_{PAM}
1.5 % < PAM ≤2.5 %	C_{PAM}
2.5 % < PAM ≤3.5 %	D_{PAM}
3.5 % < PAM ≤4.5 %	E_{PAM}
4.5 % < PAM ≤7.5 %	F_{PAM}
7.5 % ≤ PAM	G_{PAM}

Table 6
Seismic risk class of the unreinforced school building (Body A).

Parameter	Value	Class
$PGA_{Capacity}$	0.111 g	/
PGA_{Demand}	0.188 g	/
PAM	2.392 %	C
IS-V	59.0426 %	C
Seismic risk class		**C**

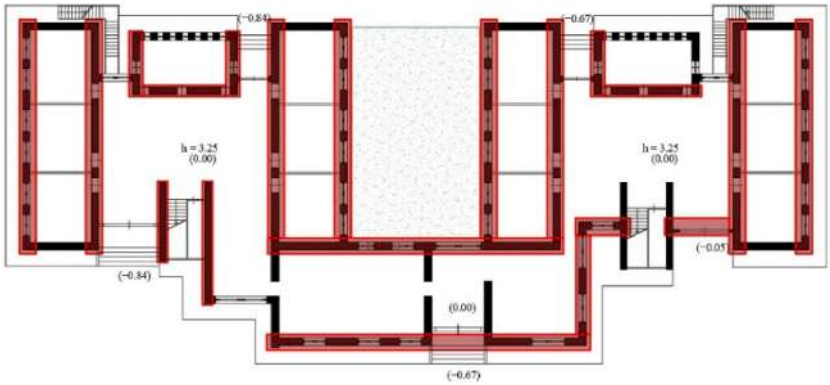

Fig. 24. Identification of the masonry walls reinforced by the considered retrofit systems.

Table 7
Mechanical properties of the H-FRP reinforcement system.

Characteristics	Value
Modulus of elasticity (E_f)	42290 N/mm^2
Ultimate design strength (f_d)	83.48 N/mm^2
Ultimate design strain (ε_d)	1.7 %

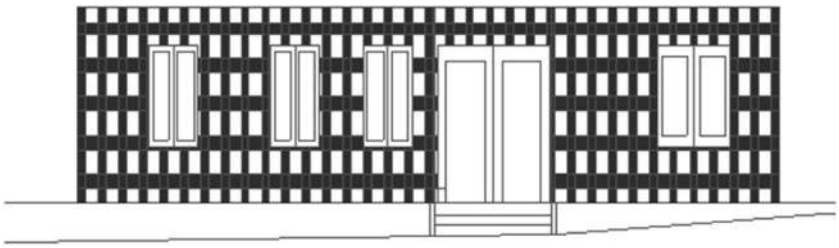

Fig. 25. FRP retrofit system applied to the school building façade.

The Italian regulations define that the seismic upgrading of an existing building is achieved when an increase of seismic risk safety index not less than 0.10 is obtained. Therefore, the H-FRP system can be considered as an efficient type of intervention to upgrade the examined school building. Nevertheless, in terms of seismic risk classification, it was not obtained any improvement. In fact, while the IS-V class changed to Class B (60 % $\leq$ IS-V $<$ 80 %), the PAM index, which decreased from 2.39 to 1.76, still fall in the range of the seismic risk class C (1.5 % $<$ PAM $\leq$2.5 %), as shown in Table 8. This means that, after the intervention, the seismic risk class of the retrofitted building is still the C one.

4.4.2. Hemp-based FRCM retrofit system

Fibre-Reinforced Cementitious Matrix (FRCM) is a retrofit system used to reinforce masonry walls. The reinforcement is made of a grid of monodirectional elements, represented in this case by hemp fibres, incorporated into a binder matrix. The main benefits deriving from using FRCM systems are related to the improvement of performances of masonry structures in terms of bending moment and shear [27]. The properties of the H-FRCM system were determined from experimental results by applying a correction factor to the compressive strength of the tuff masonry, in accordance with Italian code provisions for retrofitted masonry walls. Although the

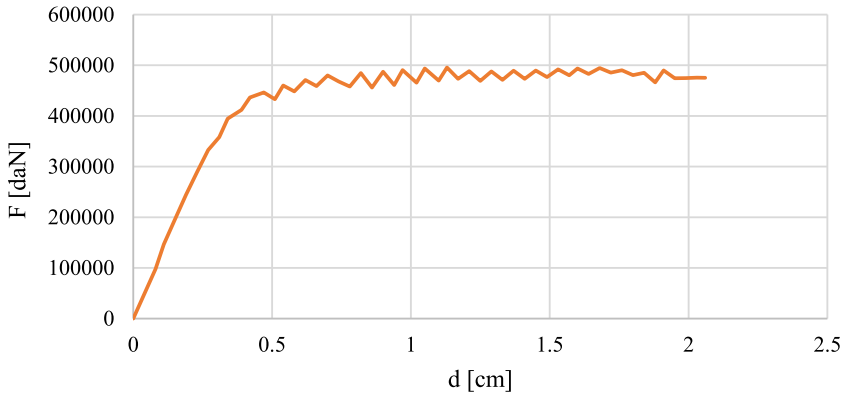

Fig. 26. Pushover curves in the most severe condition in direction X of the school building reinforced by the H-FRP system.

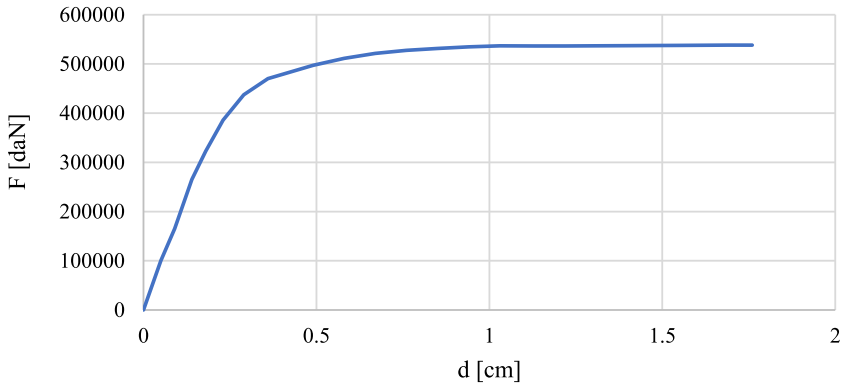

Fig. 27. Pushover curves in the most severe condition in direction Y of the school building reinforced by the H-FRP system.

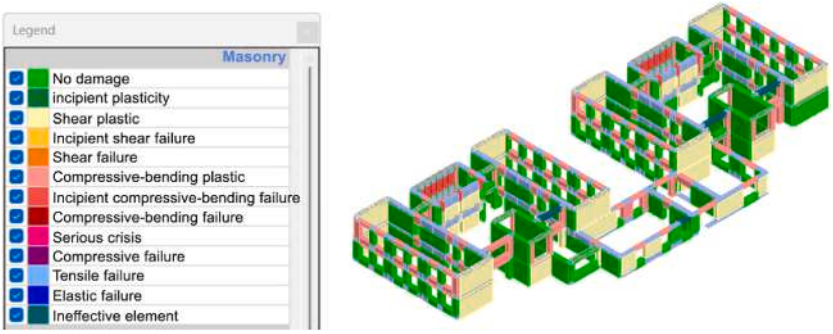

Fig. 28. Damages of the school building reinforced by the H-FRP system in the most severe load combination.

Table 8
Seismic risk class of the school building reinforced by the H-FRP system.

Parameter	Value	Class
$PGA_{Capacity}$	0.135 g	/
PGA_{Demand}	0.188 g	/
PAM	1.7554 %	C
IS-V	71.8085 %	B
Seismic risk class		**C**

standard amplification factor for mesh reinforcement is 1.5 for both tuff blocks and masonry walls, a more conservative value of 1.13 was adopted. This choice reflects the modest strength gains observed in compression tests on reinforced masonry walls and aims to more accurately capture the actual performance of the system. By using a reduced factor, the risk of overestimating the strengthening effect is minimized, especially in light of the inherent variability of the materials involved. The system was applied on the masonry structure in a single layer placed on both sides of the walls, as shown in Fig. 29.

Also in this case, the modal investigation provided similar results to those obtained on the unreinforced building. The global seismic behaviour was assessed by means of pushover analyses adopting the same 24 load combinations described for the unreinforced building. The results of the seismic analysis in terms of pushover curves in directions X and Y are illustrated in Figs. 30 and 31, respectively.

The lowest value of seismic risk safety index after the retrofit with H-FRCM systems was obtained in the X direction with a value of 0.62. This means that only an increase of 0.03 of safety index was attained compared to the unreinforced building (seismic risk safety index = 0.59). The damages occurred in the masonry walls in the most severe load combination are shown in Fig. 32.

Therefore, according to the Italian standards, it was not possible to achieve the seismic upgrading of the building. Also, in terms of seismic risk classification, no improvement of behaviour was accomplished. In fact, while the IS-V class increased to Class B (60 % $\leq$ IS-V $<$ 80 %), the PAM index, decreasing from 2.39 to 1.76, remained in the PAM range of the seismic risk class C (1.5 % $<$ PAM $\leq$2.5 %), as shown in Table 9.

A comparison between the unreinforced school building and the reinforced one in terms of seismic risk safety index (ζ_E) in the two analysis directions is summarized in Table 10. From analysis results, it was perceived that the two selected retrofit systems based on the use of hemp fibres led to a satisfactory increase of seismic performances of the existing school building, allowing to achieve the seismic upgrading only when the H-FRP system was used. However, since there was an increase of the seismic risk safety index when H-FRCM was used, this technique appears to be effective for seismic consolidation, even if much more studies must be done to improve its behaviour aiming at seismic upgrading of existing masonry constructions.

Furthermore, the shear strength of the retrofitted masonry walls in the numerical model can be evaluated using design-oriented analytical models and established technical guidelines available in the literature. Specifically, the formulations proposed by Thomoglou et al. [18] and Angiolilli et al. [19], along with the recommendations provided in the [28] and [29] guidelines, offer practical tools for estimating the shear capacity of masonry elements strengthened with inorganic matrix composite systems. These references can serve as a valuable basis for validating and supporting the numerical results obtained for the H-FRCM strengthening system examined in this study.

5. Conclusions

The research work presented in the current paper was articulated in three phases, namely two experimental laboratory campaigns to use hemp as structural reinforcement solution of masonry structures and one numerical application of two hemp-based systems for seismic reinforcement of an existing masonry building.

The first research activity was based on laboratory tests performed on a plaster reinforced with hemp fibres under forms of braids randomly added to the mixture of the pre-mixed material. The hemp braids were preliminary subjected to absorption capacity test, from which it was found that the fibres absorb around 4.5 times their weight mainly in the first two immersion hours. The consistency of each blend was assessed by means of workability test, that showed a decrease in workability as increasing the percentages of fibres. However, the values were still acceptable for a plaster with percentages of fibres lower than 1 %. The mechanical tests showed that both bending and compressive strength increased in the hemp plaster compared to the unreinforced one. The best behaviour was obtained by the mortar with 0.5 % of fibres with length of 2 cm, that reached an increase in bending and compressive strengths of around 71 % and 52 %, respectively, compared to the samples without hemp fibres. A significant result was also the observation of the confinement effect provided by the hemp fibres, that allowed to reach higher values of strain especially in the compressive tests.

The second research was still devoted to performing laboratory tests. In this case, a Fibre Reinforced Cementitious Matrix (FRCM) adopting hemp fibres was investigated. The preliminary tests on hemp braids, namely absorption capacity test and uniaxial tensile test, led to choose hemp fibres with diameter of 2 mm, that showed a water absorption capacity of 1.3 times their initial weight and an ultimate tensile strength of 68 MPa. The wall samples were tested under compression load and showed an increase in ultimate force of around 14 % for the reinforced specimen (703.8 MPa) compared to the control one (619.4 MPa) and a small increase of ultimate displacement (4.5 %). The most interesting results concerned the differences in the collapse modes. In fact, the unreinforced specimen showed several lesions in the bricks and the out-of-plane failure of the plaster, while, thanks to the hemp mesh and the used mechanical

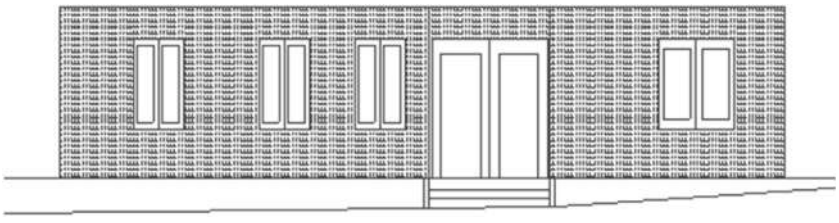

Fig. 29. H-FRCM retrofit system applied to a façade of the school building.

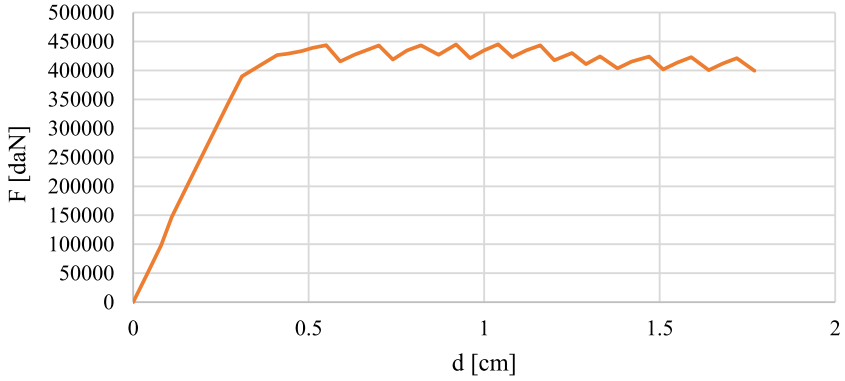

Fig. 30. Pushover curves in direction X of the school building reinforced by the H-FRCM system.

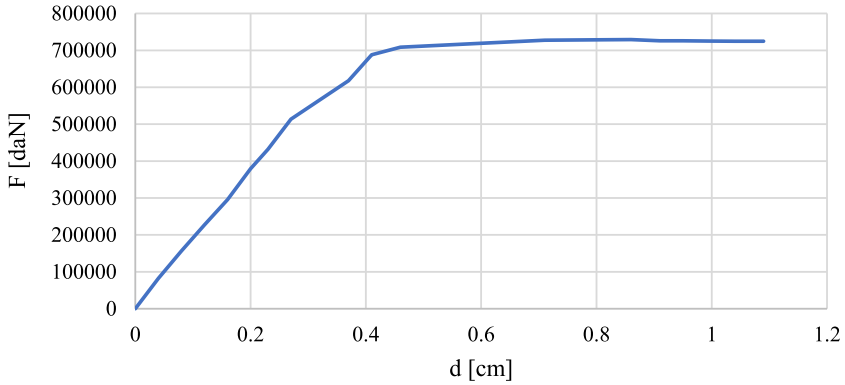

Fig. 31. Pushover curves in direction Y of the school building reinforced by the H-FRCM system.

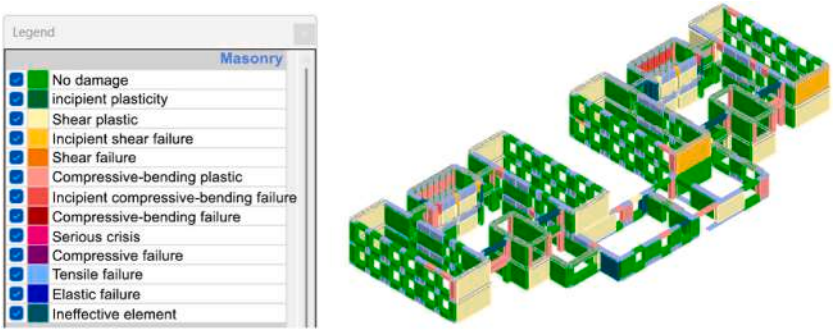

Fig. 32. Damages of the school building reinforced by the H-FRCM system in the most severe load combination.

Table 9
Seismic risk class of the school building reinforced by the H-FRCM system.

Parameter	Value	Class
$PGA_{Capacity}$	0.120 g	/
PGA_{Demand}	0.188 g	/
PAM	1.7644 %	C
IS-V	63.8298 %	B
Seismic risk class		**C**

Table 10
Comparison of the results in terms of seismic risk safety index.

Model	ζ_E dir. X	ζ_E dir. Y
Unreinforced	0.59	0.62
Reinforced_Hemp FRP	0.72	0.86
Reinforced_Hemp FRCM	0.62	0.68

anchors, in the reinforced specimen it was not observed the expulsion of the plaster, but only a capillary crack pattern, without significant lesions in the bricks.

Finally, it was performed a numerical application on a masonry school building retrofitted by two seismic strengthening systems, represented by a Hemp-based Fibre-Reinforced Polymer (H-FRP) and a Hemp-based Fibre-Reinforced Cementitious Matrix (H-FRCM). The results showed the increase of the seismic safety index ζ_E, computed according to the Italian standard (NTC 2018), for both analysed retrofit systems. Nevertheless, only using the H-FRP system the seismic upgrading of the building, with an increase of the ζ_E factor of 0.13 (from 0.59 to 0.72) was achieved. On the other hand, with the H-FRCM system only an increase of the seismic safety index of 0.03, insufficient to reach the building seismic upgrading, was attained. In both cases the seismic class computed according to the 2017 Italian Guidelines (class C) remained the same of the unreinforced school building, since the PAM index was not significantly reduced to reach a higher class.

As a conclusion, the overall results of the research are highly encouraging for the possibility of using hemp fibres for the seismic strengthening of existing masonry buildings. However, both the experimental campaign and the numerical analysis will require further investigations on a larger number of specimens and on different geometrical configurations of the reinforcement system to find the optimal technique for retrofitting existing masonry buildings, especially when H-FRCM-based solutions are of concern.

CRediT authorship contribution statement

Emilia Meglio: Software, Formal analysis, Writing – original draft, Investigation, Resources. **Antonio Formisano:** Resources, Methodology, Writing – review & editing, Supervision, Data curation, Validation, Project administration, Funding acquisition, Conceptualization.

Declaration of competing interest

The authors declare that they have no known competing financial interests or personal relationships that could have appeared to influence the work reported in this paper.

Acknowledgments

The present study is financed by the European Union – Next GenerationEU – National Plan for Recovery and Resilience (PNRR) – Mission 4 – Component 2, Investment n. 1.1., Call PRIN 2022 PNR D.D. 1409 of 14-09-2022 (RE SI LI ENT project - Waste REuse for anti-SeIsmic masonry buiLdIngs with energy-efficiENT behaviour, CUP N. E53D23017560001), which is gratefully acknowledged by the Authors.

Data availability

Data will be made available on request.

References

[1] Global Alliance for Buildings and Construction GABC, 2020 global status report. Towards a Zero-Emission, Efficient and Resilience Buildings and Construction Sector, 2020.
[2] M. Li, Y. Pu, V.M. Thomas, C.G. Yoo, S. Ozcan, Y. Deng, K. Nelson, A.J. Ragauskas, Recent advancements of plant-based natural fiber–reinforced composites and their applications, Compos. Part B Eng. 200 (2020) 108254, https://doi.org/10.1016/j.compositesb.2020.108254.
[3] E. Awwad, M. Mabsout, B. Hamad, M.T. Farran, H. Khatib, Studies of fiber-reinforced concrete using industrial hemp fibers, Constr. Build. Mater. 35 (2012) 710–717, https://doi.org/10.1016/j.conbuildmat.2012.04.119.
[4] T. Jami, S.R. Karade, L.P. Singh, A review of the properties of hemp concrete for green building applications, J. Clean. Prod. 239 (2019) 117852, https://doi.org/10.1016/j.jclepro.2019.117852.
[5] B.M. Prasad, M.M. Sain, Mechanical properties of thermally treated hemp fibers in inert atmosphere for potential composite reinforcement, Mater. Res. Innov. 7 (2016) 231–238, https://doi.org/10.1007/s10019-003-0258-y.
[6] M. Fan, Characterization and performance of elementary hemp fibres: factors influencing tensile strength, Bioresources 5 (4) (2010) 2307–2322.
[7] A. Piot, T. Béjat, A. Jay, L. Bessette, E. Wurtz, L. Barnes-Davin, Study of a hempcrete wall exposed to outdoor climate: effects of the coating, Constr. Build. Mater. 139 (2017) 540–550, https://doi.org/10.1016/j.conbuildmat.2016.12.143.
[8] D. Jones, C. Brischke, Performance of Bio-based Building Materials, Woodhead Publishing, Cambridge, United Kingdom, 2015.
[9] B. Comak, A. Bideci, O.S. Bideci, Effects of hemp fibers on characteristics of cement based mortar, Constr. Build. Mater. 169 (2018) 794–799, https://doi.org/10.1016/j.conbuildmat.2018.03.029.
[10] D. Asprone, M. Durante, A. Prota, G. Manfredi, Potential of structural pozzolanic matrix-hemp fiber grid composites, Constr. Build. Mater. 25 (2011) 2867–2874, https://doi.org/10.1016/j.conbuildmat.2010.12.046.

[11] C. Menna, D. Asprone, M. Durante, A. Zinno, A. Balsamo, A. Prota, Structural behaviour of masonry panels strengthened with an innovative hemp fibre composite grid, Constr. Build. Mater. 100 (2015) 111–121, https://doi.org/10.1016/j.conbuildmat.2015.09.051.
[12] L. Arnaud, E. Gourlay, Experimental study of parameters influencing mechanical properties of hemp concretes, Constr. Build. Mater. 28 (2012) 50–56, https://doi.org/10.1016/j.conbuildmat.2011.07.052.
[13] I. Merta, E.K. Tschegg, Fracture energy of natural fibre reinforced concrete, Constr. Build. Mater. 40 (2013) 991–997, https://doi.org/10.1016/j.conbuildmat.2012.11.060.
[14] V. Dubois, E. Wirquin, C. Flament, P. Sloma, Fresh and hardened state properties of hemp concrete made up of a large proportion of quarry fines for the production of blocks, Constr. Build. Mater. 102 (2016) 84–93, https://doi.org/10.1016/j.conbuildmat.2015.10.196.
[15] P. Zak, T. Ashour, A. Korjenic, S. Korjenic, W. Wu, The influence of natural reinforcement fibres, gypsum and cement on compressive strength of Earth bricks materials, Constr. Build. Mater. 106 (2016) 179–188, https://doi.org/10.1016/j.conbuildmat.2015.12.031.
[16] American Society for Testing and Materials, ASTM C1557: Standard Test Method for Tensile Strength and Young's Modulus of Fibers, 2008. West Conshohocken, PA, USA.
[17] A. Cascardi, F. Micelli, M.A. Aiello, Analytical modelmbased on artificial neural network for masonry shear walls strengthened with FRM systems, Compos. B Eng. 95 (2016) 252–263.
[18] A.K. Thomoglou, T.C. Rousakis, D.V. Achillopoulou, A.I. Karabinis, Ultimate shear strength prediction model for unreinforced masonry retrofitted externally with textile reinforced mortar, Earthq. Struct 19 (6) (2020) 411–425.
[19] M. Angiolilli, A. Gregori, S. Cattari, Performance of Fiber Reinforced Mortar coating for irregular stone masonry: experimental and analytical investigations, Constr. Build. Mater. 294 (2021) 123508.
[20] Ministry of Infrastructure and Transport, Circular No. 7/2019: Instructions for the Application of the New Technical Code for Constructions Nr. 35 of 11-02-2019, Official Gazette, Rome, Italy, 2019 (in Italian).
[21] S. Lagomarsino, S. Podestà, S. Resemini, E. Curti, S. Parodi, Mechanical models for the seismic vulnerability assessment of churches, in: Proceedings of the 4th International Seminar on Structural Analysis of Historical Constructions (SAHC04), Padua, Italy, 10–13 November 2004 vol. 2, Taylor & Francis, London, UK, 2004, pp. 1091–1101, 2004.
[22] A. Penna, S. Lagomarsino, A. Galasco, A nonlinear macroelement model for the seismic analysis of masonry buildings, Earthq. Eng. Struct. Dynam. 43 (2013) 159–179, https://doi.org/10.1002/eqe.2335.
[23] Ministry of Infrastructure and Transport. NTC, Technical Standards for Construction Nr. 42 of 20-2-2018, Official Gazette, Rome, Italy, 2018, 2018 (in Italian).
[24] Ministerial Decree of Infrastructures (M. D. 65, 07/03/2017)., Guidelines for the Seismic Classification of Buildings, Ministry of Infrastructure and Transport, Rome, Italy, 2017 (in Italian).
[25] A.P. Piccolo, G. Longobardi, A. Formisano, Seismic vulnerability and consolidation by FRP/FRCM systems of a masonry school building in the district of naples, Buildings 12 (2022) 2040, https://doi.org/10.3390/buildings12112040.
[26] G. Ramaglia, G. Crisci, F. Fabbrocino, G.L. Lignola, A. Prota, FRP vs FRCM in flexural strengthening of masonry, in: Proceedings of the SMAR 2019, 5th Conference on Smart Monitoring, Assessment and Rehabilitation of Civil Structures, Potsdam, Germany, 2019, pp. 27–29. August 2019.
[27] G. Amato, J.F. Chen, J. D'Anna, L. La Mendola, G. Minafò, FRCM systems for strengthening masonry structures, in: Proceedings of the 8th Biennial Conference on Advanced Composites in Construction, 2017. Sheffield, UK, 5–7 September 2017.
[28] CNR-DT 215/2018. National Research CouncilGuide for the Design and Construction of Externally Bonded Externally Bonded Matrix Systems for Strengthening Existing Structures. Rome - CNR June 30th, 2020.
[29] ACI 549.6R-20, Guide to Design and Construction of Externally Bonded Fabric-Reinforced Cementitious Matrix (FRCM) and Steel-Reinforced Grout (SRG) Systems for Repair and Strengthening Masonry Structures, 2020.